

The Role of Patina on Archaeological Copper Alloy Coins in the Outbreak and Progression of Bronze Disease

Johanna C. Thunberg*
Cardiff University
Cardiff, UK
thunbergjc@cardiff.ac.uk

David E. Watkinson
Cardiff University
Cardiff, UK
watkinson@cardiff.ac.uk

Nicola J. Emmerson
Cardiff University
Cardiff, UK
emmersonnj@cardiff.ac.uk

Zoltan Kis
Centre for Energy Research
Budapest, Hungary
kis.zoltan@energia.mta.hu

Ildikó Harsányi
Centre for Energy Research
Budapest, Hungary
harsanyi.ildiko@energia.mta.hu

Zsolt Kasztovszky
Centre for Energy Research
Budapest, Hungary
[kastovszky.zsolt@energia.mta.hu](mailto:kasztovszky.zsolt@energia.mta.hu)

Mark Lewis
National Roman Legion Museum
Caerleon, UK
mark.lewis@museumwales.ac.uk

*Author for correspondence

Abstract

Archaeological copper alloy objects form unique corrosion structures according to their manufacture and burial environment. Categorisation has identified protective Type I structures and chloride-containing Type II structures which may lead to bronze disease. Using visual examination to determine which of these exist on objects dictates conservation decisions; unfortunately, there is limited evidence linking surface features directly to corrosion risk. In this study, the chloride content of 39 archaeological copper alloy coins was determined non-destructively using prompt gamma-ray activation analysis. Their surfaces

were examined through Raman spectroscopy, reflective transformation imaging and visually using descriptors reflecting Type I, Type II and ‘bronze disease’ surfaces. When subjected to high relative humidity, none of the coins exhibited bronze disease despite containing chlorides and showing characteristics of Type II structures. The results highlight the difficulty of determining risk and taking informed decisions for the management of archaeological copper alloy objects.

Keywords

bronze disease, corrosion monitoring, management, decision-making, conservation, characterisation

Introduction

Archaeological copper alloy objects often occur in large numbers in heritage collections. The primary concern with these objects is the onset of bronze disease. This is an active, chloride-driven corrosion process that can result in the complete destruction of an object (Scott 2002). Bronze disease develops from cuprous chloride (CuCl), which forms adjacent to the metal core during burial when chloride ions interact with cuprous ions (1) (Wang et al. 2006):



If $\text{pH} < 5$, cuprous oxide (Cu_2O) can also form CuCl through (2) (Grayburn et al. 2015):



In a post-excavation environment, CuCl can interact with atmospheric oxygen and moisture to form copper trihydroxychloride isomers ($\text{Cu}_2(\text{OH})_3\text{Cl}$) (3) (Dowsett et al. 2012):



The rapid and voluminous growth of $\text{Cu}_2(\text{OH})_3\text{Cl}$ can disrupt overlying corrosion layers, destroying surface details and forming a disfiguring growth on the surface. The ability of the process to continuously form CuCl (4) means that the destruction will continue until the supply of oxygen, atmospheric moisture or copper is suppressed (MacLeod 1981).



As a result of the significant risks to objects suffering from bronze disease, conservation efforts are focused on preventing post-excavation processes from occurring.

Management of archaeological copper alloys

The tools to evaluate the risk of bronze disease within practical or ethical restraints are limited. Thorough investigation of the burial and post-excavation environments, and the nature of the alloy, manufacturing processes and corrosion stratigraphy can inform conservation strategies, but this information is rarely available. The location of CuCl next to the metal surface means that it cannot be identified without destructive sampling. Due to the complex formation of corrosion products, surface analysis offers limited insight unless $\text{Cu}_2(\text{OH})_3\text{Cl}$ is detected, yet at this point the object is likely to have already incurred damage. In practice, visual inspection is often employed for assessing the condition of copper alloy objects. The success

of visual inspection is dependent on factors such as understanding of corrosion processes, experience, colour perception and method of assessment. Guidance to identify active corrosion can standardise and improve the accuracy of assessments.

Archaeological copper alloys display complex corrosion profiles as a result of extrinsic factors, such as the chemo-physical properties of the burial environment, and intrinsic factors, such as the nature of the alloy and manufacturing processes (Ingo et al. 2019, Leygraf et al. 2019). The appearance of copper alloy objects can therefore differ widely. Despite this, it has been suggested that copper alloys can fall within two types of corrosion structures that create distinguishable features, commonly recognised as Type I and Type II structures (Robbiola et al. 1998). A literature review of conservation and archaeometallurgical publications identified over 50 sources applying Type I or Type II structures to characterise objects, suggesting they are often used for this reason. A Type I structure has a two-layered profile that replicates the metal surface ('original surface') without a significant change in volume. A Type II structure is defined by a porous, three-layer profile rich in chloride ions next to the metal and containing no detail from the original surface. As a result of their corrosion history, Type I and Type II structures could display features that are visually distinguishable by their textures and colours. Being able to separate these surfaces by appearance is potentially important for conservation practice, as a Type I structure is believed to have protective properties, while a Type II structure is thought unstable due to its chloride content and by allowing ion transport (Payer et al. 1995, Robbiola et al. 1998).

Examination of guidelines and literature reveals the existence of jargon in conservation practice to describe archaeological copper alloy surfaces and bronze disease, with many terms overlapping or being closely connected to the terminology used by Robbiola et al. (1998) to define Type I and Type II patinas (e.g. Wadsak et al. 2000, Constantinides et al. 2002, Bozzini et al. 2017, Cosano et al. 2018). Table 1 demonstrates the descriptors most frequently encountered in literature to describe Type I and Type II patinas, alongside descriptors used to identify bronze disease (Table 1). Several descriptors to identify bronze disease overlap those with a Type II patina, indicating that these may be linked.

Insert Table 1 here.

While the terminology around archaeological copper alloys is well established, the link between the descriptors in Table 1 and the stability of an object has not been investigated in detail. When copper alloy objects in the Burrell collection were examined in a recent study, only 6 of the 64 objects suspected to suffer from bronze disease after visual inspection were shown to be actively corroding (Bryan 2021). This suggests that the accuracy of descriptors currently used in practice to identify objects affected by bronze disease is low.

As object appearance informs conservation decision-making, it is critical to have a good understanding of the information that can be determined visually from corroded surfaces. This pilot-study explores the link between existing vocabulary to describe copper alloy objects and the outbreak of bronze disease.

Aim and objectives

This study aims to investigate the relationship between the appearance of archaeological copper alloy objects, the presence of chlorides and the risk of bronze disease. This is achieved by:

- characterising the surfaces of 39 Roman archaeological copper alloy coins by visual and instrumental analysis
- establishing the chloride content of the coins by prompt gamma-ray activation analysis (PGAA)
- exposing the coins to high humidity environments understood to trigger bronze disease and monitoring corrosion using reflectance transformation imaging (RTI) and oxygen consumption

Method

In this study, 39 archaeological copper alloy coins (IP01–IP40) were examined (Figure 1). These were metal detectorist finds donated to Cardiff University Conservation Department for research. The coins varied between 6 and 27 mm in diameter and weighed between 0.88 and 4.96 g. X-radiography demonstrated that all of the coins had a metallic core. The detection site and context are unknown, and the coins are therefore deemed of low archaeological value. The coins were mechanically cleaned to remove soil products.

Insert Figure 1 here.

Establishing chloride content

The bulk chloride content of the coins was determined non-destructively using PGAA at Budapest Neutron Centre, Hungary. PGAA can detect bulk chloride through irradiation from a cold-neutron beam which detects characteristic gamma-photons emitted in (n, γ) reactions. The neutrons can penetrate several centimetres into a material, facilitating determination of the bulk concentration of elements in small objects. The distribution of chlorides was mapped in three coins (IP05, IP39 and IP40) using the NIPS–NORMA (neutron-induced prompt gamma-ray spectroscopy–neutron optics and radiography for material analysis) station.

Surface examination

All coins were recorded using a Broncolor Scope D50 RTI dome equipped with 48 white (5000 K \pm 75 K) LED lights. Images were processed using Truvis Authentica software. Images were captured with a Nikon D5600 with a Nikon AF-S Micro-Nikkor 105 mm lens.

Raman spectroscopy was employed to characterise surface corrosion products with a B&W Tek iRaman Plus equipped with a 785 nm (resolution $\sim 3.5 \text{ cm}^{-1}$ max 30 mW) and 532 nm (resolution $\sim 4.5 \text{ cm}^{-1}$ max 340 mW) probe at $\times 50$ magnification (laser spot size 42 μm). Integration time ranged from 2 to 60 sec and 1 to 100 acquisitions. Laser intensity ranged from 1% to 5% of maximum laser output. Twenty spectra of each coin were taken at sites of different colours and textures to account for the surface heterogeneity of the coins.

Three trained conservators with practical experience of working with archaeological copper alloys examined the surface of each coin at $\times 4$ magnification under a Just Normlicht XL colour viewing light with a D65 LED light source (colour temperature of 6500 K) at a 70 cm working distance. The descriptors in Table 1 were used to characterise the surface of each coin during examination. All descriptors that were applicable to describe the surface of the coins were selected.

Corrosion monitoring

Coins IP01–IP40 were subjected to a saturated humidity environment and monitored for any physical signs of active corrosion for 37 days. A 100% relative humidity (RH) environment was created by enclosing three beakers with cotton wool saturated with water (total 450 mL) in a Stewart Gastronorm 13l polypropylene box.

The oxygen consumption of five coins containing the highest chloride content (IP05, IP11, IP39, IP20 and IP40) was measured individually to produce a quantitative measure of their corrosion rates. The method has been reported in detail in an open access publication (Emmerson et al. 2021).

A 250 mL Mason Ball jar was used to create an airtight environment for oxygen measurements containing a two-point PreSens GmbH SP-PSt3-NAU-D5-YOP ruthenium oxygen sensor spot adhered to the interior wall using Radio Spares RTV silicone rubber compound. Every vessel was assigned a Madgetech RHTemp101A datalogger ($\pm 1.1\%$ RH at 80% RH) to monitor the internal RH. Silica gel conditioned to 80% RH was enclosed in the vessel to maintain a high humidity environment for the test duration. A relative humidity of 80% RH was chosen as a suitable environment to detect activity related to bronze disease as this is known to produce rapid corrosion rates (Thickett 2016). A PreSens GmbH POF-L2.5-1SMA 505 nm fibre sensor connected to a Fibox 4 oxygen meter was used as the luminescence source. The coins were monitored for their oxygen consumption for 44 days.

To investigate the protective properties of corrosion structures, coins IP05, IP11, IP20, IP39 and IP40 were thereafter scored through the corrosion profile and down to the metal surface using a scalpel, revealing the full corrosion profile of the coin and potentially exposing chloride sites (Figure 2). Their oxygen consumption was recorded for 140 days. Detailed mapping of chlorides using NIPS–NORMA on IP05, IP11 and IP39 determined the location of scoring down the middle of the obverse and reverse of the coins (Figure 2). All coins were visually assessed at the end of oxygen consumption to control for any changes.

Insert Figure 2 here

Results

PGAA/NIPS–NORMA analysis

The chloride content in all of the coins is expressed as a ratio of chloride to copper in elemental weight. All of the coins (IP01–IP40) contained chloride, demonstrating a copper to chloride ratio between 2.65×10^{-4} and 1.46×10^{-2} (Figure 3). Neutron imaging of IP05, IP11 and IP39 demonstrated that chloride was localised within the coin.

Surface examination

During examination, different descriptors were employed by each observer to characterise a coin. No two coins had identical sets of descriptors, and descriptors for Type I, Type II and bronze disease were used to describe each coin (Figure 3). The five coins with the highest chloride/copper ratio (IP05, IP11, IP20, IP39, IP40) and those with the lowest chloride/copper ratio (IP01, IP24, IP25, IP30, IP36) were characterised by many overlapping descriptors, with no apparent distinguishing features to suggest one set would contain more chlorides (Figure 4).

Eighteen coins displayed some preservation of the original surface detail. These were both within the range of the highest (IP05, IP20, IP39, IP40) and lowest (IP01, IP25) chloride-containing coins, demonstrating no obvious relationship between the preservation of the original surface detail and chloride content (Figure 3).

Insert Figure 3 here

Insert Figure 4 here

Some descriptors were used consistently throughout the dataset, whereas some were never used to describe surface features (Table 2).

Insert Table 2 here

Detection of corrosion compounds using Raman spectroscopy was difficult, probably due to poor crystallinity of the corrosion products and significant fluorescence masking the Raman signal. Raman detected the presence of malachite ($\text{Cu}_2\text{CO}_3(\text{OH})_2$) and cerussite (PbCO_3) (Figure 5). Soil components included quartz, calcite, feldspar and the TiO_2 isomers rutile and anatase.

Insert Figure 5 here

Corrosion monitoring

None of the coins showed signs of active corrosion after exposure to 100% RH. Coins IP05, IP11, IP39, IP20 and IP40 did not consume any oxygen during exposure to 80% RH. Scoring the coins to damage the patina did not affect their oxygen consumption rate, and the coins did not develop any visible signs of bronze disease.

Discussion

Establishing the presence of chloride cannot indicate whether bronze disease will occur. None of the coins investigated developed new signs of active corrosion when subjected to environments known to promote the process, despite a known chloride content. Compromising the patina and exposing chloride sites in five of the coins with the highest chloride content (IP05, IP11, IP39 and IP40) did not result in the break out of bronze disease. This makes it unlikely that any CuCl was exposed during the study.

It is possible that the chlorides mapped by PGAA and NIPS–NORMA are not present as CuCl but located elsewhere in the corrosion products. Copper trihydroxychlorides ($\text{Cu}_2(\text{OH})_3\text{Cl}$) may already be present in the patina, and other copper chloride compounds, such as connellite ($\text{Cu}_{19}\text{Cl}_4(\text{SO}_4)(\text{OH})_{32}\cdot 3(\text{H}_2\text{O})$), sampleite ($\text{NaCaCu}_5(\text{PO}_4)_4\text{Cl}\cdot 5(\text{H}_2\text{O})$) and calumetite ($\text{Cu}(\text{OH}, \text{Cl})_2\cdot 2(\text{H}_2\text{O})$), have been found on archaeological copper alloys (Scott 2002, Giovanelli et al. 2010, Muros and Scott 2018). Other alloying chloride compounds have been identified, such as mendipite ($\text{Pb}_3\text{Cl}_2\text{O}_2$), pyromorphite ($\text{Pb}(\text{PO}_4)_3\text{Cl}$) and laurionite ($\text{PbCl}(\text{OH})$) in leaded copper alloys (Ingo et al. 2006, Bernard and Joiret 2009, Mezzi et al. 2012) and AgCl in silvered coins (Fabrizi et al. 2019). None of these compounds were identified using Raman spectroscopy, but due to the heterogeneity of the surface, poor crystallinity of compounds and the limit of laser penetration, these compounds could still be present. Chlorides could also be present as a soil product and integrated on the surface. A

second, follow-up study will examine the coins in more detail to locate chlorides throughout the corrosion profiles.

Surface examination

The surface examination of each coin using descriptors highlights the subjectivity of visual examination and the difficulty of standardising vocabulary to guide object inspection. Several challenges occurred during examination resulting in an unclear relationship between surface features and chloride content, further limiting the ability to correlate the appearance of objects to risk. These challenges included:

- Interpretation of key descriptors
A range of descriptors were not used by assessors due to the lack of references illustrating the descriptors, making them difficult to interpret. Others lacked a contrasting reference point, such as ‘soft’ or ‘underweight’. The challenge of using descriptors to characterise a surface is demonstrated in the range of terminology used by the assessors to characterise the same objects.
- Applicability of descriptors for each object
Interpretation of object surfaces is further complicated by the presence of Type I, Type II and bronze disease descriptors on all examined surfaces. While this reflects the heterogeneity of archaeological copper alloy surfaces, it suggests that there is a limit to the usefulness of these descriptors for categorising them. This is illustrated in Figure 6, which shows the similarity of a stable surface (IP03) and the surface of a coin from a different sample set on which active bronze disease has been recorded.

Insert Figure 6 here

- Insufficient terminology to reflect the complexity of some surfaces
Despite the range of terminology used to distinguish Type I, Type II and bronze disease surfaces, the descriptors did not reflect the complexity of each coin. In particular, colour may not be a reliable indicator owing to the colourant properties of Cu(II), which may produce a range of products similar in colour (Leygraf et al. 2019), as illustrated in Figure 6.

Implications for conservation practice

Identifying chloride in archaeological copper alloy corrosion structures is not a determining factor in identifying risk of bronze disease. Consequently, visual examination and identification of surface features that are suggestive of a chloride-containing corrosion structure may not be a reliable indicator that bronze disease will occur. Complexity of surfaces, ambiguity in interpretation of descriptors and the occurrence of multiple features on the surface of one object will further complicate decision-making.

Some key features that were not used by the assessors in this study could be indicators of bronze disease (Table 2) but may only provide retrospective evidence for ongoing active corrosion when damage has already occurred, rather than detect risk. As the outbreak of bronze disease may not occur immediately after excavation, active bronze disease can proceed unhindered unless objects are monitored regularly. Conversely, the cautious approach of bulk treatment or environmental control of objects (possibly unnecessarily) to

mitigate the risk of bronze disease can be costly in time, materials and potential exposure to harmful materials and may also result in unwanted surface alterations.

Conclusion

- This study highlights the limitations of using visual examination and surface analysis to determine whether an object is at risk of developing bronze disease, which normally dictates management policy and treatment decisions.
- Using written guidance for visual analysis is complex, and it is difficult to determine the success of using descriptors.
- Some terminology may be more useful for determining the risk of active bronze disease, but a more precise language is necessary to determine risk.
- Non-destructive analysis techniques to determine the presence of chlorides are of limited use in assigning risk, as they do not serve as an indicator for bronze disease.
- The cost-benefit rationale for treatment or implementing environmental control is affected when corrosion risk cannot be evidenced.
- Ongoing monitoring to detect changes in copper alloys on display or in storage is an important but often monumental task.

The sample set of coins are of similar size, dimension and corrosion thicknesses and cannot provide a complete picture of the different corrosion surfaces associated with bronze disease. A further larger-scale study will include objects of different shapes and contexts to gain a more complete understanding of appearance/bronze disease relationships. A follow-up study is underway to determine the chloride location throughout the corrosion profiles of the coins.

Acknowledgements

The authors wish to thank the AHRC-funded SWW DTP consortium and IPERION CH for supporting this project.

References

- Bernard, M.C. and S. Joiret. 2009. Understanding corrosion of ancient metals for the conservation of cultural heritage. *Electrochimica Acta* 54: 5199–205.
- Bozzini, B., B. Alemán, M. Amati, M. Boniardi, V. Caramia, G. Giovannelli, L. Gregoratti, and M. Kazemian Abyaneh. 2017. Novel insight into bronze disease gained by synchrotron-based photoelectron spectro-microscopy, in support of electrochemical treatment strategies. *Studies in Conservation* 62(8): 465–73.
- Bryan, B.N. 2021. Copper alloy objects suspected of bronze disease – The Burrell ‘Bronzes’. In *Studies in archaeological conservation*, eds. C. Caple and V. Garlick, 115–23. London: Routledge.
- Constantinides, I., A. Adriaens, and F. Adams. 2002. Surface characterization of artificial corrosion layers on copper alloy reference materials. *Applied Surface Science* 189: 90–101.
- Cosano, D., D. Esquivel, L.D. Mateos, F. Quesada, C. Jiménez-Sanchidrián, and J.R. Ruiz. 2018. Spectroscopic analysis of corrosion products in a bronze cauldron from the Late

Iberian Iron Age. *Spectrochimica Acta Part A: Molecular and Biomolecular Spectroscopy* 205: 489–96.

Dowsett, M., A. Adriaens, C. Martin, and L. Bouchenoire. 2012. The use of synchrotron X-rays to observe copper corrosion in real time. *Analytical Chemistry* 84: 4866–72.

Emmerson, N.J., J.H. Seifert, and D.E. Watkinson. 2021. Refining the use of oxygen consumption as a proxy corrosion rate measure for archaeological and historic iron. *European Physical Journal Plus* 135: art. 546.

Fabrizi, L., F. Di Turo, L. Medeghini, M. Di Fazio, F. Catalli, and C. De Vito. 2019. The application of non-destructive techniques for the study of corrosion patinas of ten Roman silver coins: The case of the medieval *Grosso Romanino*. *Microchemical Journal* 145: 419–27.

Giovanelli, G., L. D'Urzo, G. Maggiulli, S. Natali, C. Pagliara, I. Sgura, and B. Bozzini. 2010. Cathodic chloride extraction treatment of a late Bronze Age artifact affected by bronze disease in room-temperature ionic-liquid 1-ethyl-3-methylimidazolium bis(trifluoromethanesulfonyl)imide (EMI-TFSI). *Journal of Solid State Electrochemistry* 14: 479–94.

Grayburn, R., M. Dowsett, M. Hand, P.-I. Sabbe, P. Thompson, and A. Adriaens. 2015. Tracking the progression of bronze disease. *Corrosion Science* 91: 220–23.

Ingo, G.M., T. De Caro, C. Ruccucci, E. Angelini, S. Grassini, S. Balbi, P. Bernardini, D. Salvi, L. Bouselmi, A. Cilingiroglu, M. Gener, V.K. Gouda, O. Al Jarrah, S. Khosroff, Z. Mahdjoub, Z. Al Saad, W. El-Saddik, and P. Vassilou. 2006. Large scale investigation of chemical composition, structure and corrosion mechanism of bronze archaeological artefacts from Mediterranean basin. *Applied Physics A* 83: 513–20.

Ingo, G.M., C. Ruccucci, G. Guida, M. Albin, C. Giuliani, and G. Di Carlo. 2019. Rebuilding of the burial environment from the chemical biography of archaeological copper-based artifacts. *ACS Omega* 4: 11103–111.

Leygraf, C., T. Chang, G. Herting, and I. Odnevall Wallinder. 2019. The origin and evolution of copper patina colour. *Corrosion Science* 157: 337–46.

Macleod, I. 1981. Bronze disease: An electrochemical explanation. *ICCM Bulletin* 7(1): 16–26.

Mezzi, A., E. Angelini, C. Ruccucci, S. Grassini, T. De Caro, F. Faraldo, and P. Bernardini. 2012. Micro-structural and micro-chemical composition of bronze artefacts from Tharros (Western Sardinia, Italy). *Surface and Interface Analysis* 44: 958–62.

Muros, V. and D. Scott. 2018. The occurrence of brochantite on archaeological bronzes: A case study from Lofkend, Albania. *Studies in Conservation* 63(2): 113–25.

Payer, J.H., G. Ball, B.I. Rickett, and H.S. Kim. 1995. Role of transport properties in corrosion product growth. *Materials Science and Engineering: A* 198 (1–2): 91–102.

Robbiola, L., J.-M. Blengino, and C. Fiaud. 1998. Morphology and mechanisms of formation of natural patinas on archaeological Cu-Sn alloys. *Corrosion Science* 40(12): 2091–111.

Scott, D.A. 2002. *Copper and bronze in art: Corrosion, colorants, conservation*. Los Angeles: The Getty Conservation Institute.

Thickett, D. 2016. Critical relative humidity levels and carbonyl pollution concentrations for archaeological copper alloys. In *Metal 2016: Proceedings of the Interim Meeting of the ICOM-CC Metals Working Group, 26–30 September 2016*, eds. R. Menon, C. Chemello, and A. Pandya, 180–87. New Delhi: International Council of Museums-Committee for Conservation (ICOM-CC) and Indira Gandhi National Centre for the Arts (IGNCA).

Wadsak, M., I. Constantinides, G. Vittiglio, A. Adriaens, K. Janssens, M. Schreiner, F.C. Adams, P. Brunella, and M. Wuttmann. 2000. Multianalytical study of patina formed on archaeological metal objects from Bliesbruck-Reinheim. *Microchimica Acta* 133: 159–64.

Wang, J., C. Xu, and G. Lv. 2006. Formation processes of CuCl and regenerated Cu crystals on bronze surfaces in neutral and acidic media. *Applied Surface Science* 252(18): 6294–303.

Authors

Johanna C. Thunberg teaches conservation and is undertaking a PhD at Cardiff University. Her research focuses on storage protocols for archaeological metals and identification of instability in copper alloy artefacts.

David E. Watkinson teaches and researches conservation at Cardiff University. His work on the corrosion rate of iron underpins the preservation of Brunel’s iron steamship SS *Great Britain*.

Nicola J. Emmerson lectures in conservation science at Cardiff University and researches the management of corrosion prevention strategies for metallic cultural heritage artefacts.

Zoltan Kis is a senior fellow scientist at the Centre for Energy Research, specialising in gamma spectroscopy, PGAA and imaging.

Idikó Harsányi is a researcher at the Centre for Energy Research. She has published extensively on the use of PGAA to examine archaeological materials.

Zsolt Kasztovszky is a senior fellow scientist at the Centre for Energy Research, focusing on nuclear chemistry and applications of PGAA in archaeometry and material sciences.

Mark Lewis is a senior curator at the National Roman Legion Museum, National Museum Wales and an expert in Roman archaeology.

Table 1. Example of descriptors used in literature to characterise archaeological copper alloys

Table 2. Descriptors applied to all coin surfaces and descriptors not used to characterise coin surfaces



Figure 1. Images of all coins examined. Images are not to scale. Length of diameter at widest point is given in mm in parentheses

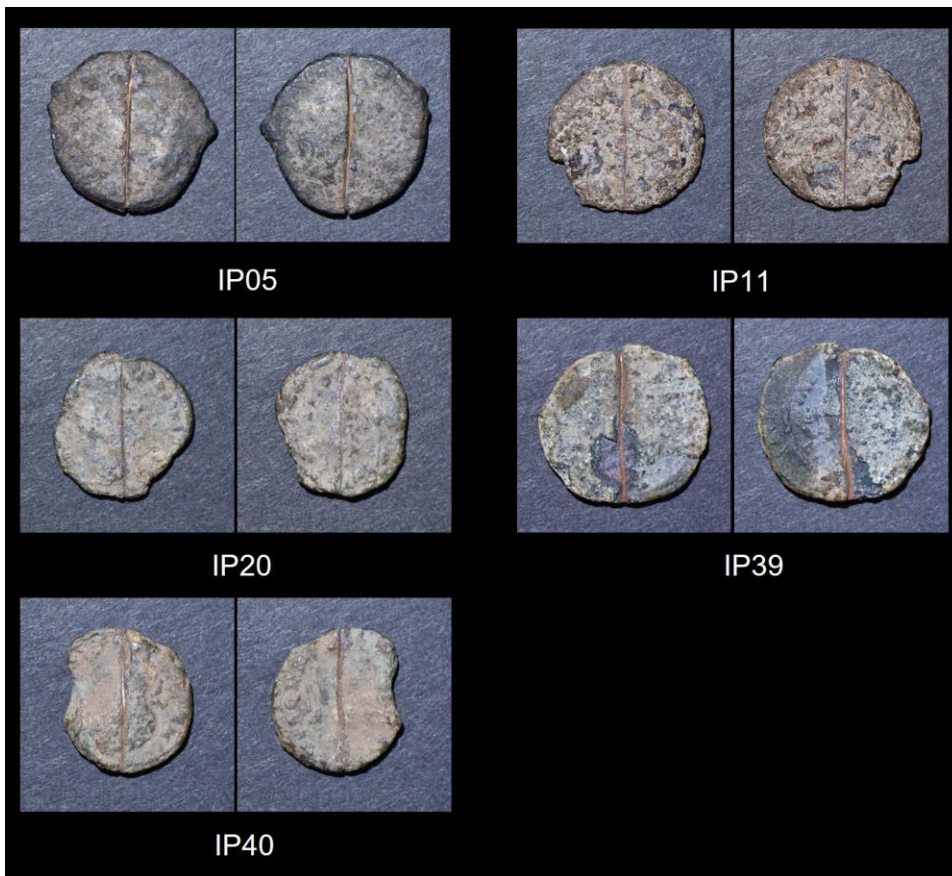


Figure 2. IP05, IP11, IP20, IP39 and IP40 after scoring on the obverse and reverse

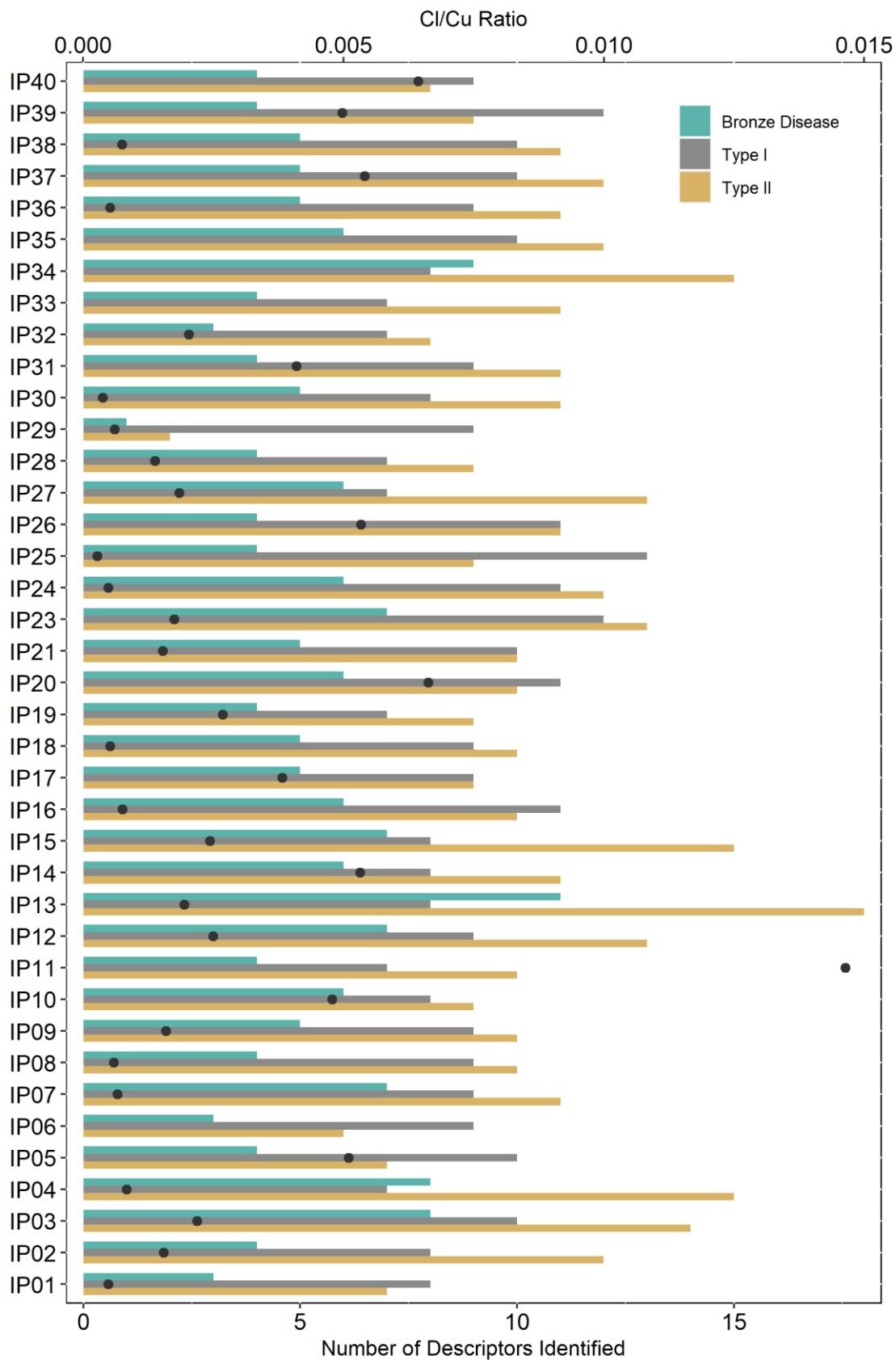


Figure 3. The number of Type I patina, Type II patina and bronze disease characteristics identified in each coin by at least one of the three assessors. The chloride/copper ratio of each coin as measured by PGAA is included

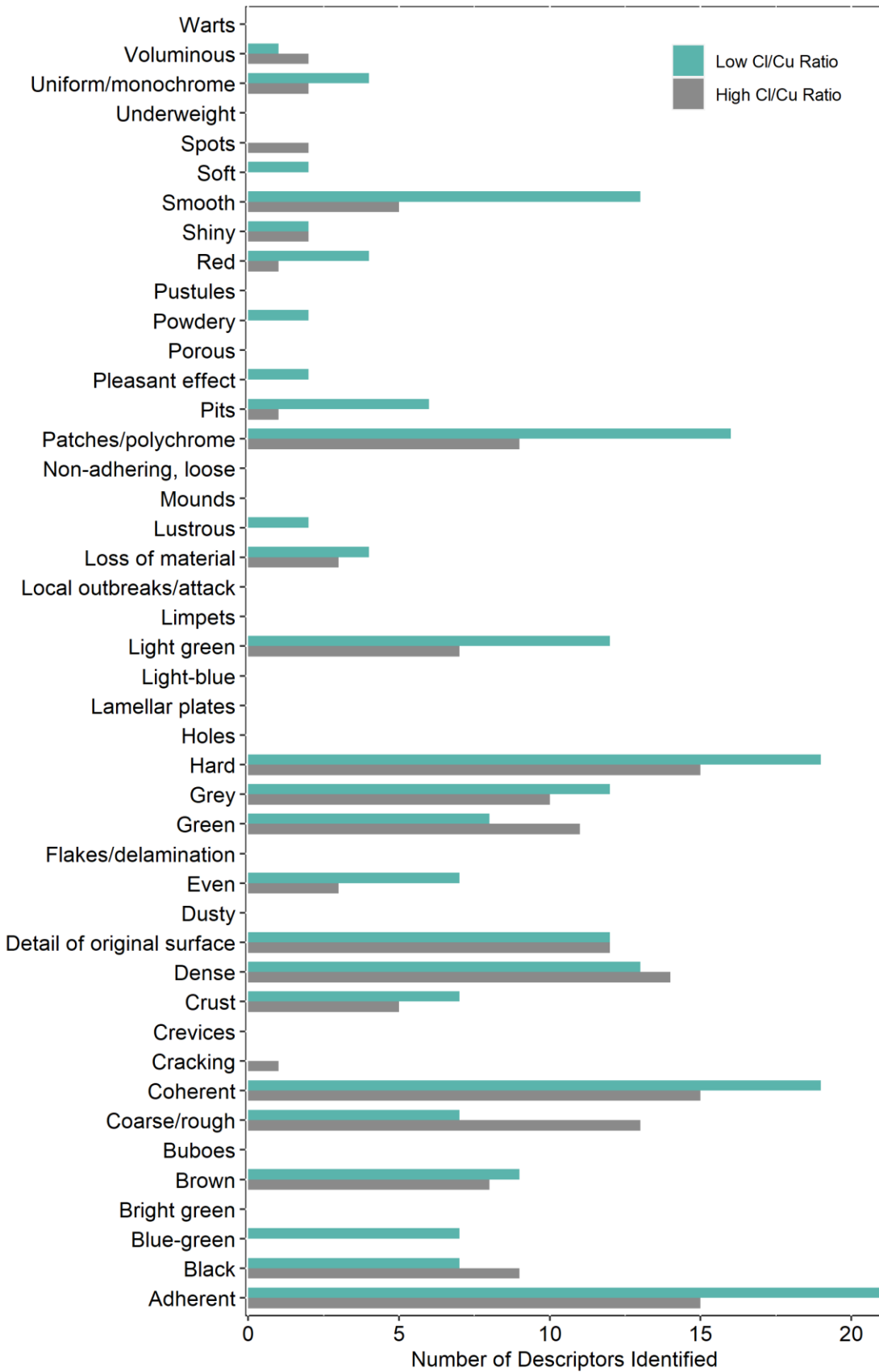


Figure 4. Descriptors used for the coins containing the lowest chloride content (IP01, IP24, IP25, IP30 and IP36) and highest chloride content (IP05, IP11, IP20, IP39 and IP40)

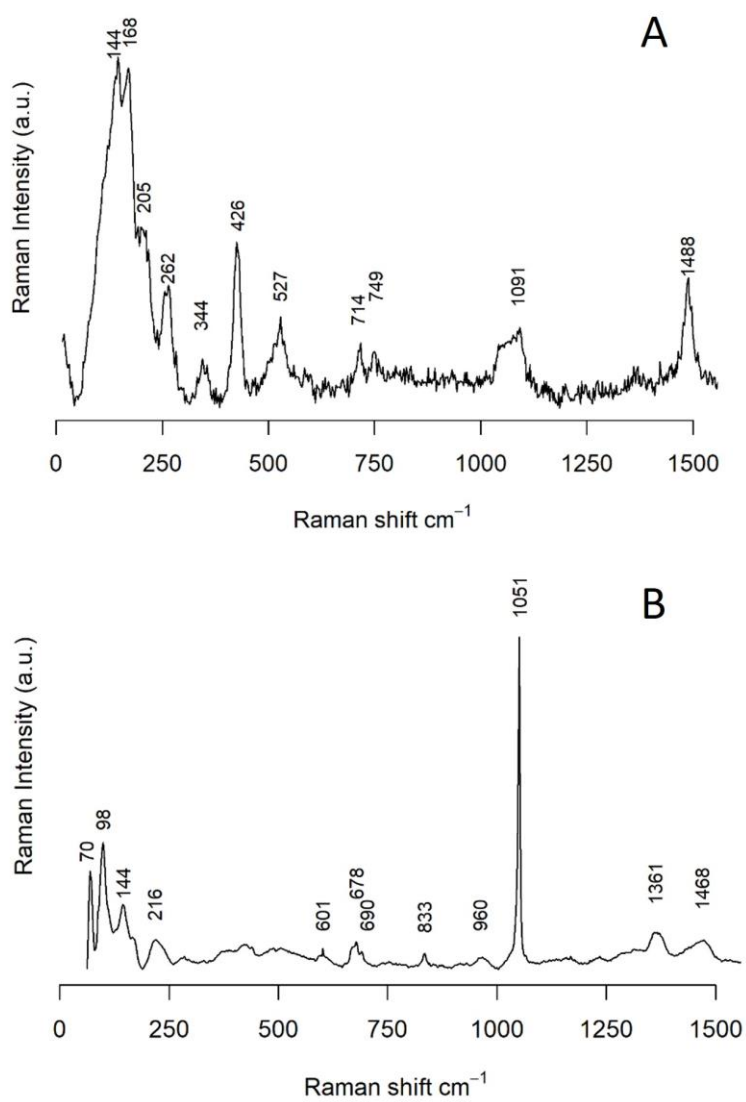


Figure 5. Raman spectra of (a) malachite ($\text{Cu}_2\text{CO}_3(\text{OH})_2$) and (b) cerussite (PbCO_3)



Figure 6. IP03 (\varnothing 10.6 mm) and an actively corroding coin (\varnothing 25.9 mm) from outside this sample set showing similarity of surface features

	Type I	Type II	Bronze disease
Texture	Smooth	Powdery	Powdery
	Even	Buboes	Dusty
	Uniform/monochrome	Warts	Patches
	Shiny	Limpets	Flakes
	Lustrous	Coarse/rough	Blisters
	Hard	Pits	Warts
	Dense	Crevices	Pustules
	Pleasant effect	Crust	Mounds
	Coherent	Loss of material (incl. spalling, breakup of overlying layers)	Loss of material
	Adherent	Local outbreaks/attack	Voluminous
	Compact	Patches	Local outbreaks/attack
	Detail from original surface	Polychrome	Spots
		Spots	Cracking
		Cracking	Non-adhering, loose
		Soft	Pits
		Non-adhering, loose	
		Underweight	
		Lamellar plates	
		Flakes/delamination	
		Holes	
	Porous		
	Hard to nearly hard		
	No detail from original surface		
Colour	Green	Green	Green
	Red	Light green	Blue–green
	Brown	Light blue	Pale green
	Grey	Bright green	Bright green
	Blue	Blue–green	Light green
		Black	
		Red	
	Brown		

Table 1. Example of descriptors used in literature to characterise archaeological copper alloys

Descriptors used for all coins	Descriptors not used
Hard	Soft
Dense	Porous
Coherent	Dusty
Adherent	Warts
	Pustules
	Buboes
	Limpets
	Cracking
	Holes
	Pleasant effect

Table 2. Descriptors applied to all coin surfaces and descriptors not used to characterise coin surfaces